arXiv:cond-mat/0208287v1 [cond-mat.soft] 14 Aug 2002

Smectic ordering in liquid crystal - aerosil dispersions II. Scaling analysis

Germano S. Iannacchione
Department of Physics, Worcester Polytechnic Institute, Worcester, Massachusetts 01609, USA

Sungil Park* and Carl W. Garland
School of Science, Massachusetts Institute of Technology, Cambridge, Massachusetts 02139, USA

Robert J. Birgeneau
Department of Physics, University of Toronto, Toronto, Ontario M5S 1A1 Canada

Robert L. Leheny
Department of Physics and Astronomy, Johns Hopkins University, Baltimore, Maryland 21218, USA

(Dated: February 1, 2008)

Liquid crystals offer many unique opportunities to study various phase transitions with continuous symmetry in the presence of quenched random disorder (QRD). The QRD arises from the presence of porous solids in the form of a random gel network. Experimental and theoretical work support the view that for fixed (static) inclusions, quasi-long-range smectic order is destroyed for arbitrarily small volume fractions of the solid. However, the presence of porous solids indicates that finite-size effects could play some role in limiting long-range order. In an earlier work, the nematic - smectic-A transition region of octylcyanobiphenyl (8CB) and silica aerosils was investigated calorimetrically. A detailed x-ray study of this system is presented in the preceding Paper I, which indicates that pseudo-critical scaling behavior is observed. In the present paper, the role of finite-size scaling and two-scale universality aspects of the 8CB+aerosil system are presented and the dependence of the QRD strength on the aerosil density is discussed.

PACS numbers: 64.70.Md,61.30.Eb,61.10.-i

I. INTRODUCTION

The study of the effect of quenched random disorder (QRD) on phase transitional behavior remains an attractive area of research due to the broad implications outside the laboratory. The underlying physics has applications ranging from unique assemblies of complex fluids to doped semiconductors. Many systems have been the focus of both theoretical and experimental studies. The experimental efforts have concentrated on idealized model systems in the hopes of isolating the essential features of quenched random disorder. They include the still enigmatic superfluid transition of ^{4}He in aerogels and porous glasses, the superfluid transition and phase separation of ^{4}He-^{3}He mixtures in silica aerogels [1] and doped magnet systems [2]. Relatively recent efforts with liquid crystal (LC) - silica composites [3, 4, 5, 6, 7, 8, 9] have demonstrated that these are especially interesting model systems. They are of particular importance as a way to access "soft" (elastically weak) phases of continuous symmetry, which are directly coupled to surfaces and external fields.

The general consensus is that the physics of QRD in liquid crystals is essentially contained by a Random-Field approach [10]. Recent theoretical efforts predict that an Ising system with quenched random fields will move towards a new Random-Field Ising (RFI) fixed point with increasing disorder. However, a Random-Field XY ($RFXY$) system has no new fixed point that is stable. Here, with increasing strength of the disordering random field, an $RFXY$ system still has flows toward the XY fixed point until long-range order is destroyed [10]. Thus one expects, in general, that a $3D$-XY system subject to random-field perturbations has no true long-range order (LRO). A detailed theoretical study of QRD effects on smectic ordering in liquid crystals [11] concludes that arbitrarily small amounts of QRD destroy even quasi-LRO and hence, no true smectic phase exists since the smectic correlation length remains finite for all strengths of disorder and all temperatures. This theoretical conclusion is in agreement with a recent x-ray study of octylcyanobiphenyl (8CB)+aerosil dispersions [8], the detailed results of which are presented in the companion paper to this work, denoted hereafter as paper I [12]. This x-ray study reveals a finite, though large, smectic correlation length for all temperatures and densities of silica. However, smectic thermal fluctuations still exist above a pseudo nematic to smectic transition at T* (close to but below T^o_{NA} for pure 8CB). These smectic fluctuations are expected to remain in the XY universality class but also show crossover behavior from Gaussian tricritical (TC) to $3D$-XY with increasing strength of disorder [12].

In all fluid systems studied to date as models of such QRD effects, including the liquid crystal system mentioned above, the random perturbations are introduced via the embedding of a random (gel-like) solid structure into the phase ordering material. An open question remains as to the connection between the concentration of such solid inclusions and the strength of the random disordering field. Also, the identification of QRD is complicated by finite-size effects which could, in principle, play a dominant role in such systems. In simple finite-size scaling (FSS), where the confining surfaces play no interactive role, the *bulk* critical correlation fluctuations are cut-off at a length dictated by the distance between surfaces, which corresponds to a minimum reduced temperature where the transition is "truncated". However, when the surfaces are arranged in a random manner with high void connectivity in order to introduce QRD, the distance between surfaces no longer acts as an upper length scale in the system, and changes in the transition's critical behavior may also occur. Given the absence of LRO in such perturbed systems, the required characterization of the critical behavior may not be possible. In spite of this, if a critical power-law analysis of the transition heat capacity data is available, then, through two-scale universality, the critical behavior of the correlation length for $T > T^*$ may be estimated and compared with direct measurements. Finally, if the introduced random surfaces have in addition the freedom of an elastic response, then coupling between the gel and host elasticities can occur. This latter effect has only begun to be explored theoretically [13, 14, 15].

---

*Present Address: NCNR, NIST, Gaithersburg, MD.

The particular system that is the focus of this paper is a silica colloidal gel of aerosil particles dispersed in a liquid crystal denoted as LC+aerosil. The analysis will also be applied to another, earlier, system of an aerogel (fused silica gel) structure embedded within a liquid crystal denoted as LC+aerogel. The two are nearly identical in every respect −− fractal-like nature of the gel structure, surface chemistry, and density −− save for their relative elasticity. Additionally, the ease at achieving nearly arbitrary silica densities for the aerosil system allows for greater control of the disorder. For the 8CB+aerosil system, thermal evidence for two regimes of behavior has been found [4]: low-density gels where pseudo-critical behavior is closely related to that for the pure LC and higher density gels where all transition features appear to be smeared. More rigid aerogels in LC+aerogel systems are crudely like the LC+aerosil gels in the high density regime but differ in some important ways since the elastic strain imposed by the random anchoring surfaces of aerogels is fully quenched. It appears that the disorder introduced by an aerogel is so great that all "transition" features are dramatically smeared and the physics of such systems may be more closely related to static random-elastic strain disorder.

In spite of the loss of smectic LRO, Paper I [12] and an earlier calorimetric study of 8CB+aerosils [4] show that smectic thermal fluctuations still play an important role in LC+aerosil systems. Many concepts from pure materials such as finite-size scaling, two-scale universality, and tricritical-to-XY crossover due to variable de Gennes coupling need to be considered in addition to intrinsic new quenched random effects that dominate at temperatures below an effective transition temperature. The present paper is organized as follows. The relevant characteristics of an aerosil gel are described in Section II. Section III reviews the essential features of LC+aerosil behavior near the N-SmA transition. The application of scaling analysis to calorimetric and x-ray results on the 8CB+aerosil system is presented in Section IV with comparisons made to the 8CB+aerogel system. Section V summarizes the conclusions that can be drawn from such scaling analysis and discusses the issue of the relationship between the RF strength and the aerosil density. Appendix A reviews the relevant N-SmA critical behavior in pure liquid crystals, and Appendix B presents the necessary background for two-scale universality and finite-size scaling.

II. GENERAL DESCRIPTION OF AEROSIL GELS

For liquid crystal systems, the introduction of quenched random disorder typically requires the inclusion of random solid surfaces. This can be accomplished by the percolation of a low-volume-fraction gel structure randomly arranged throughout the LC host. Such gels can be physically realized by a diffusion-limited-aggregation process which forms fractal-like structures having a wide distribution of void length scales. In practical terms, the fractal-like character is limited to length scales much larger than the size of the basic unit and smaller than some macroscopic size limiting the gel, i.e., the sample size.

Because of the hydroxyl groups on the surface of the 70 Å diameter hydrophilic aerosil (SiO_2) spheres used in this work, hydrogen-bonding is possible between aerosil particles [16]. When dispersed in an organic liquid medium, aerosil particles comprising 3 to 4 lightly fused spheres and having a mean radius of gyration of ≈ 240 Å [4] will attach to each other and form a gel by a diffusion-limited aggregation process. This gel can be thought of as a randomly crossing "pearl necklace" of silica and a cartoon depiction is given in Fig. 1. The hydrogen-bonded nature of the silica "links" is relatively weak and gives these gels the ability to break easily and reform on moderate time scales (such gels are termed thixotropic). In addition, because of the diffusion-limited aggregation process by which gelation occurs, the structure of the final gel may become anisotropic if the gelation occurs in an anisotropic fluid, i.e., gelation in a well aligned nematic or smectic liquid crystal. This gives such colloidal gels very attractive uses in future research as a route to studying anisotropic random disorder [17].

These aerosil gels are very similar in structure to the well-known and previously studied aerogels, which are another type of fractal silica gel. Aerogels are formed by a reaction-limited aggregation process and form a gel nearly identical to that of aerosils except that the ba-

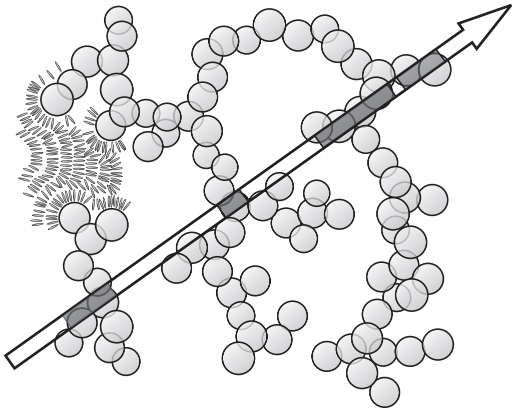

FIG. 1: Circles and "hairs" (upper left) represent type-300, 70 Å diameter, aerosil particles and 8CB molecules, respectively, drawn to approximate scale. This cartoon corresponds to an average void length $l_o \approx 400$ Å and $\rho_S \approx 0.20$, where the density units are grams of silica per cm^3 of 8CB. The solid volume fraction is $\Phi \approx 0.08$. Open and shaded parts of arrow depict void and solid chords respectively.

sic silica units in aerogels are chemically fused together. Thus, aerogels have a large shear modulus (they break before yielding) while in contrast aerosil gels have a quite small, density-dependent, shear modulus [18]. Thus, aerosil gels can respond elastically to strains, which may turn out to be a crucial difference as will be discussed later. For the present work, the thixotropic character ensures that the silica strands mainly dictate, at low silica concentrations, the local nematic director without imposing high-energy elastic strains over the material throughout the void. As the silica density increases, the aerosil gel eventually becomes stiff enough to elastically strain the host fluid.

For any random gel structure, a mean distance between solid (gel) surfaces or a mean void size, l_o, can be uniquely defined despite the wide distribution of void sizes. The definition of l_o in terms of macroscopic, and experimentally accessible, quantities begins by imagining a "straw" of uniform cross-section A sent through the gel; see Fig. 1. The places where the gel randomly intersects the "straw" defines a solid length while the distance between intersections defines a void length. The relevant macroscopic quantities are the specific surface area a in total surface area per mass (given as 300 m^2 g^{-1} [16] for the type R300 aerosil used in the 8CB+aerosil samples) and the reduced density, $\rho_S =$ mass of solid per open volume or in our case grams of silica per cm^3 of LC. Since the cross-section of this imaginary straw is uniform, the proper summing of the total void and solid volumes of the straw depends only on the void and solid lengths respectively, noting that each void must be bounded by two walls. The sum of the total solid length and the total void length is simply the length of the straw which spans the sample.

The two requirements for volume and length defined above allow the definition of the average void length as

$$l_o = 2/a\rho_S \; . \tag{1}$$

See Ref. [4] and [19] for a more detailed derivation. Strictly speaking, this definition of l_o is valid only in the dilute regime where the addition of more solid does not significantly change the specific surface area. However, as the concentration of solid increases, more surface area is lost due to multiple connections ("clumping" of basic units); thus the specific surface area should be a decreasing function of the solid volume fraction Φ. A limiting case of interest is when completely enclosed pores occur. Here, the open volume is now bounded on all sides and a re-derivation of the mean void (now pore) size along the lines described above yields $l_o = 6/a\rho_S$. This can be recast into the form given in Eq. (1) if $a_{pore} \rightarrow a_{void}/3$. Thus, Eq. (1) is quite general for a random gel structure if the variation of a with ρ_S is known. The exact variation of a with solid concentration depends on the specific process of densification of the gel. Since the gel structures for both aerosil gels and aerogels are nearly identical, results for void sizes determined from small-angle x-ray scattering (SAXS) of various density aerogels [20] can be used to estimate the variation of $a(\rho_S)$, in m^2 per gram, as $a = 300 - 103.8\rho_S$, where ρ_S has the units grams of SiO$_2$ per cm^3 of LC. The condition for closed pores is crudely predicted to occur at $\rho_S \approx 1.97$ g cm^{-3} (assuming a continuous process of diffusion-limited aggregation). For all LC+aerosil and LC+aerogel samples studied to date, the density of silica employed has been well below that limit and the use of this estimate of $a(\rho_S)$ in Eq. (1) reproduces quite closely the SAXS measured void sizes of aerogels. This provides some confidence that a useful representation of a characteristic length scale l_o for fractal-like gels is available.

From the above discussion, the reduced density ρ_S is an attractive quantity to describe the gel and its disordering character [21]. Note that the volume fraction of LC in a silica boundary layer of thickness l_b is given by p = $l_b a \rho_S$ [4]. This quantity p is the fraction of LC filling the voids that is in direct contact with the solid surfaces and thus considered strongly "pinned". Since p is a natural measure of the "disordering strength" of the gel, ρ_S is expected to be linearly related to this QRD strength for low to moderate ρ_S values [22].

III. NEMATIC - SMECTIC-A BEHAVIOR FOR LIQUID CRYSTAL - SILICA DISPERSIONS

The essential feature of importance here is the observation that low silica density LC+aerosil samples exhibit pseudo-critical behavior that is parallel to the critical behavior exhibited by pure LCs in spite of the absence of smectic long range order in LC+aerosils. In Paper I, the usual scaling concepts are shown to hold for the relationship between the normalized thermal fluctuation amplitude σ_1^N and the parallel correlation length $\xi_\parallel$ for T > T*, where T* is an effective N-SmA transition temperature. These concepts also hold for the temperature dependence of the normalized integrated area of the static (QRD) fluctuation term in the x-ray structure factor for T < T*, where this area is proportional to a_2^N, and we drop hereafter the superscript N denoting normalization. In the latter case, it is shown in Paper I that $a_2 \sim (\mathrm{T}^* - \mathrm{T})^x$, where the "critical" exponent x is essentially the same as 2β for the smectic order parameter squared in pure liquid crystals. Calorimetric data for 8CB+aerosils [4] support this view that effective critical behavior occurs for low silica density LC+aerosil samples.

The background given in App. A for trends in N-SmA critical behavior for pure liquid crystals as a function of the McMillan ration R_M =$\mathrm{T}_{NA}/\mathrm{T}_{NI}$ is pertinent to LC+aerosil systems. It appears that increasing the density ρ_S of the thixotropic gel of aerosils decreases the smectic-nematic coupling described in App. A. Indeed, there is a simple empirical connection between the variable R_M for pure LCs and the variable ρ_S for LC+aerosils. As described in Section IV of Paper I, an effective McMillan ratio R_M^{eff}(sil) for LC+aerosil systems can be defined as

$$R_M^{eff}(\mathrm{sil}) = 0.977 - 0.47\rho_\mathrm{S} \ . \tag{2}$$

Figure 11 in Paper I demonstrates this equivalence of R_M and ρ_S as measures of changes in the smectic-nematic coupling in pure LCs and LC+aerosils. This connection will be discussed further in Sec. IVB.

The full power-law form in terms of the reduced temperature t =|T−T* | / T* used to analyze experimental specific heat data associated with the N-SmA phase transition is [23]

$$\begin{aligned}\Delta C_p(NA) &= C_p(\mathrm{observed}) - \mathrm{C_p}(\mathrm{background}) \\ &= A^{\pm} t^{-\alpha}(1 + D^{\pm} t^{\Delta_1}) + B_c \ , \end{aligned}\tag{3}$$

where the critical behavior as a function of reduced temperature t is characterized by an exponent α, an amplitude $A^{\pm}$ above and below the transition, a critical background term B_c, and corrections-to-scaling terms characterized by the coefficients $D^{\pm}$ and exponent $\Delta_1 \simeq 0.5$. The excess N-SmA specific heat (heat capacity per gram of LC) data for 8CB+aerosil samples [4] is reproduced in Fig. 2 in log-log form in order to illustrate the quantities described above. Figure 2 highlights the quality of the fits to the standard power-law form for 8CB+aerosil samples with low ρ_S. Note the importance of the inclusion of the corrections-to-scaling term, seen as curvature at high t. In fact the quality of the fit for the lowest density 8CB+aerosil sample rivals that observed for most pure LCs. In addition, the changing shape of the N-SmA heat capacity peak with ρ_S is clearly evident. As discussed in Ref. [4], it is clear from Fig. 2 that a fit to the data with Eq. (3) can include only data for | t |>| $t_m^{\pm}$ | since the ΔC_p peak is truncated at a finite maximum value $h_M \equiv \Delta C_p^{max}(NA)$.

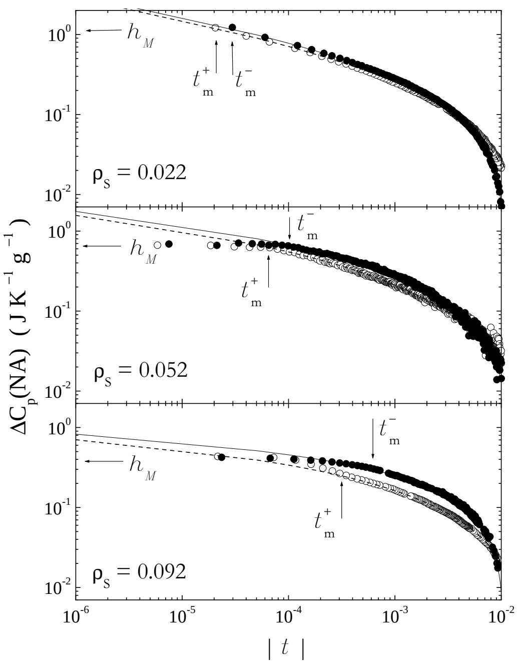

FIG. 2: Specific heat due to the N-SmA phase transition, $\Delta C_p(NA)$, as a function of reduced temperature t, for three 8CB+aerosil samples with aerosil densities ρ_S = 0.022, 0.052, and 0.092. Data taken from Ref. [4]. Open circles and dashed lines represent data and fit for $t > 0$ (above transition) while filled circles and solid lines represent data and fit for $t < 0$ (below transition). Fits were made using Eq. (3). Also indicated for each sample are $h_M \equiv \Delta C_p^{max}(NA)$ and the minimum reduced temperatures $t_m^{\pm}$ for which the data can be fit with a power-law.

The role of pseudo-critical behavior for the 8CB+aerosil system is fully described in Paper I and Ref. [4]. In the present paper, the applicability of two-scale universality and finite-size scaling in describing the pseudo-critical behavior in LC+aerosils is investigated. Essential scaling background material is introduced in App. B, and these concepts are implemented in Sec. IV for the analysis of the N-SmA "transition region" for 8CB+aerosils.

IV. ANALYSIS OF THE NEMATIC - SMECTIC-A TRANSITION IN THE 8CB+SIL SYSTEM

A. Specific heat behavior

In order to utilize the scaling analysis described in App. B, the maximum length scale ξ_M and the appropriate critical fluctuation parameters must be substituted into Eqs. (B3) and (B4), which are repeated here for convenience

$$\delta T^*/T^* \approx 2t_m^+ = 2(\xi_M/\xi_{\parallel o})^{-1/\nu_\parallel} \tag{4}$$

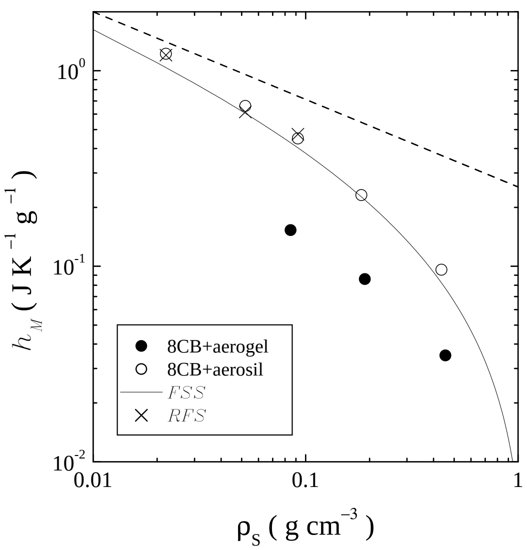

FIG. 3: Truncation plot of $h_M \equiv \Delta C_p^{max}(NA)$ versus ρ_S for 8CB+aerosils [4] and 8CB+aerogels [20]. Both the dashed and solid lines are FSS predictions based on using bulk 8CB critical parameters $\xi_{\|o}$ and $\nu_\|$ to find the reduced temperature where $\xi_M = l_o$. The dashed line represents the simple FSS result based on using only the leading singularity in Eq. (5); see text. The solid line denotes FSS using the full heat capacity function. The ×s are based on a RFS analysis using two-scale predicted critical parameters (see text) and $\xi_M = \xi_\|^{LT}$ found in Paper I.

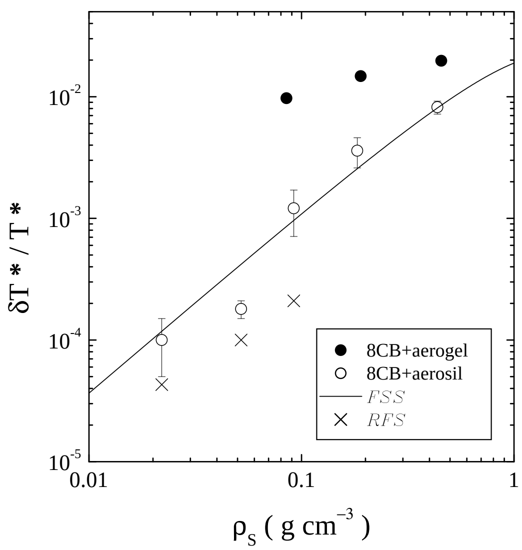

FIG. 4: Dependence on ρ_S of the fractional round-off region (gap about T*) where C$_p$ power laws fail. The solid line depicts FSS predictions using bulk critical parameters and the fluctuation cut-off length, $\xi_M = l_o$, while the ×s depict RFS predictions using two-scale critical parameters and $\xi_M = \xi_\|^{LT}$ from Paper I.

$$h_M = A^{\pm}(\xi_M/\xi_{\|o})^{\alpha/\nu_\|}(1 + D^{\pm}(\xi_M/\xi_{\|o})^{-\Delta_1/\nu_\|}) + B_c \;, \tag{5}$$

to describe the fractional temperature rounding of the transition and the specific heat maximum, respectively. In this paper, two approximations will be explored. In the first case, we use the mean void size as the cut-off length scale $\xi_M = l_o$ and the *bulk* critical parameters are used. This approach represents conventional finite-size scaling, denoted as FSS, where the cut-off length scale is set by a natural length of the "confinement". In the second case, we use the calorimetrically determined 8CB+aerosil critical parameters and two-scale predictions for the bare correlation length and exponent and set the cutoff length scale to the saturated parallel smectic correlation length found by the x-ray analysis in Paper I, i.e., $\xi_M = \xi_\|^{LT}$. This analysis recognizes that the random-field effects truncate the growth of order and tests whether two-scale universality is obeyed on approaching this truncation. We label this approach random-field scaling, or RFS for short.

The specific heat maximum $h_M \equiv \Delta C_p^{max}(NA)$ is plotted versus ρ_S in Fig. 3 for 8CB+aerosil and 8CB+aerogel samples. Given as a dashed line on this log-log plot is the simple scaling prediction using only the leading singularity of the pure 8CB heat capacity and the mean-void size as the truncation length. This ignores the critical background and corrections-to-scaling terms in Eq. (5) and yields a straight line having a slope of $\alpha/\nu_\| = 0.45$. This is the usual theoretical FSS prediction for h_M, and its failure highlights the importance of using the full expression given by Eq. (5). Surprisingly, the full analysis denoted as FSS, which uses the pure 8CB critical parameters and $\xi_M = l_o$ from Eq. (1), appears to work very well over the entire range of ρ_S. This is surprising since the critical behavior of the 8CB+aerosil samples is changing with ρ_S as seen in Fig. 2 and the saturated parallel smectic correlation length $\xi_\|^{LT}$ is much larger than l_o for all ρ_S [12]. Thus, we are suspicious that this agreement may be accidental.

The analysis denoted as RFS uses the evolving specific heat critical behavior and two-scale universality predictions (see App. B) for the equivalent correlation length critical behavior at each ρ_S. The low-temperature experimentally measured saturated parallel correlation length $\xi_\|^{LT}$ is used as the truncation length ξ_M. This analysis reproduces very closely the observed heat capacity maximum and is completely consistent with both the effective critical behavior and the maximum smectic correlation length. Unfortunately, this analysis is only applicable up to $\rho_S \approx 0.1$ since a critical analysis of $\Delta C_p(NA)$ is not possible for larger ρ_S [4]. Note that h_M for 8CB+aerogel samples can not be described by either scaling methods. For either scaling approximation to reproduce the aerogel results, a far smaller ξ_M is required, which indicates that the aerogel has a much stronger disordering influence than the aerosil at any given ρ_S value.

The fractional rounding of the transition δT*/T* for 8CB+aerosil and 8CB+aerogel samples is given versus

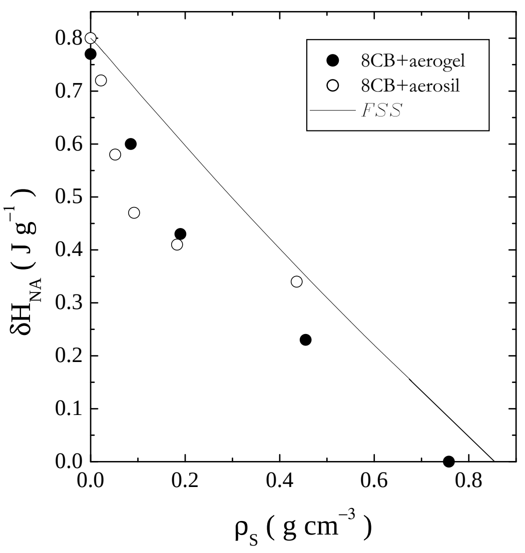

FIG. 5: The ρ_S dependence of the N-SmA transition enthalpy $\delta H_{NA} = \int \Delta C_p(\mathrm{NA})dT$. As before, filled and open circles are data taken from [20] and [4], respectively. The solid line depicts FSS using bulk 8CB critical parameters and $\xi_M = l_o$.

ρ_S in Fig. 4. For samples where critical specific heat fits were not possible, i.e., 8CB+aerosil for $\rho_S > 0.1$ and all 8CB+aerogel samples, the fractional rounding is estimated ad hoc as $\approx 10\%$ larger than the width between inflection points in ΔC_p. As was seen in Fig. 3, the FSS analysis works well for *all* densities of 8CB+aerosil samples. As before, this is surprising given the known changes in critical behavior and the fact that $\xi_{\parallel}^{LT} > l_o$. The RFS analysis predicts a somewhat sharper transition than is observed. The observed rounding is not likely influenced by the amplitude of temperature oscillations employed by the ac-calorimetric technique in Refs. [4] and [20], which is on the order of 5 mK and would account for a fractional rounding of only $\sim 10^{-5}$. The estimation $t_m^- = t_m^+$ explicit in Eq. (4) may be in question as it assumes that the unknown critical behavior of the correlation length below T* is the same as that above T*. A consequence of these arguments is that the agreement of FSS is likely accidental although intriguing. Again, the 8CB+aerogel fractional rounding is much larger than that for the 8CB+aerosil samples, which is an indication that a smaller ξ_M is required and supports the view of a stronger disordering influence for the aerogel than the aerosil.

Figure 5 presents the N-SmA transition enthalpy δH_{NA} versus ρ_S for 8CB+aerosil and 8CB+aerogel samples. Unlike h_M and δT*/T* which are measures of truncation effects on ΔC_p very close to the peak at T*, $\delta H_{NA} = \int \Delta C_p(NA)dT$ is sensitive to both truncation and changes in the shape of ΔC_p over its entire temperature range. This is clearly seen in Fig. 2 and is discussed in detail in Ref. [4]. A finite-size scaling analysis for δH_{NA} proceeds by integrating the available ΔC_p critical form approximately $\pm$3 K about T* ($|t| \approx 10^{-2}$) to the point corresponding to $t_m^{\pm}$. As an approximation, a linear evolution of ΔC_p between t_m^+ and t_m^- is assumed. The FSS analysis, given by the solid line in Fig. 5, does not agree well with the data for either system. The failure of this model is not surprising since it ignores any changes in the ΔC_p critical parameters such as $A^{\pm}$ and α with ρ_S. A RFS analysis would not be very meaningful for δH_{NA} since for $\rho_S < 0.1$, the input parameters for this model automatically insure perfect agreement. Also, the necessary input critical parameters cannot be obtained for 8CB+aerosil samples with $\rho_S > 0.1$ or for any of the 8CB+aerogel samples.

B. Smectic-A x-ray scattering for T > T*

Two-scale universality is reviewed in App. B, where it is assumed that the $3D$-XY result

$$\alpha A^+(\xi_{\parallel o}\xi_{\perp o}^2) \simeq 0.647 \qquad (6)$$

should hold for 8CB+aerosil samples. To proceed further, two additional assumptions are adopted that are inherent in the x-ray analysis presented in Paper I: ($\nu_{\parallel} - \nu_{\perp}$) and ($\xi_{\parallel o}/\xi_{\perp o}$) for 8CB+sil samples have the pure 8CB values of 0.16 and 2.22 respectively for all ρ_S. For those 8CB+aerosil samples where critical $\Delta C_p(NA)$ fits are available, the three above assumptions allow the prediction of $\xi_{\parallel o}$, $\xi_{\perp o}$, $\nu_{\parallel}$, and $\nu_{\perp}$. These parameters will vary somewhat with ρ_S since the α and A$^+$ values from the critical heat capacity fit vary with ρ_S. The resulting $\xi_{\parallel}(\rho_S$, T) "critical" behavior for T > T* permits the RFS calculations of h_M and δT*/T* presented Sec. IVA.

Given two-scale universality and the assumptions outlined above, both the bare smectic correlation length and the effective critical exponent may be estimated from the critical analysis of the heat capacity data. Thus, the self-consistent critical behavior predicted here can be directly compared to those measured in Paper I.

Presented in Fig. 6 are the experimentally measured $\xi_{\parallel}$ values as a function of reduced temperature for the 8CB+aerosil data taken from Paper I [12]. The two lines given in Fig. 6 show the observed critical behavior in pure 8CB [24], where T$_c$ is used for T*, and the two-scale prediction for $\xi_{\parallel}$ for the 8CB+aerosil sample where the predicted correlation lengths differ most from those of 8CB ($\rho_S = 0.092$). Note that although $\nu_{\parallel}$ and $\xi_{\parallel o}$ both vary with ρ_S, the predicted overall trends of $\xi_{\parallel}(t) = \xi_{\parallel o}t^{-\nu_{\parallel}}$ values differ only slightly from pure 8CB. The experimental $\xi_{\parallel}(t)$ data for various ρ_S agree well with each other within the scatter but all 8CB+aerosil values are consistently *larger* than scaling prediction. The significance of this observation is not known.

As an analog to Figure 11 of Paper I, the experimentally measured heat capacity exponents α for the N-SmA transition in pure LCs and the effective exponents α_{eff}

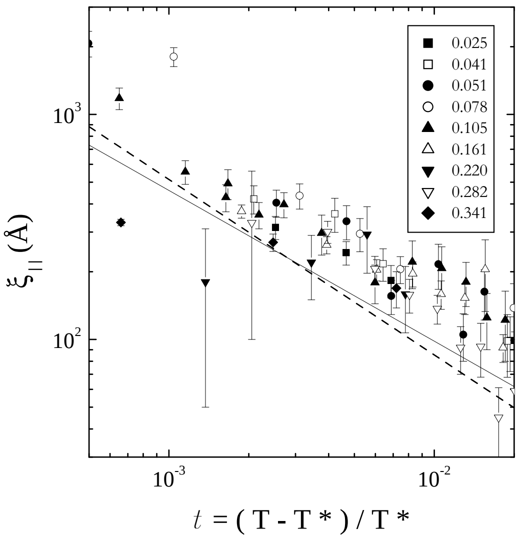

FIG. 6: Parallel smectic correlation lengths $\xi_{||}$ measured in Paper I as a function of reduced temperature t for 8CB+aerosil samples with densities ρ_S given in g cm^{-3} shown in the inset. The dashed line represent pure 8CB behavior [24] while the solid line represents the most extreme 2-scale predicted behavior for a 8CB+aerosil sample (see text).

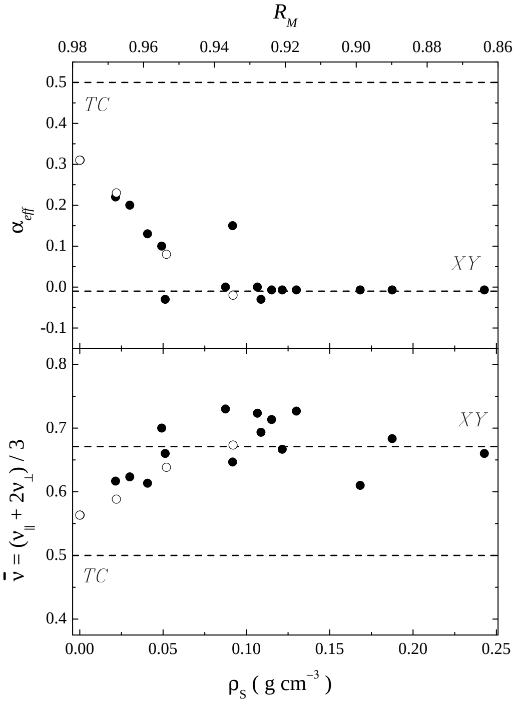

FIG. 7: Effective heat capacity critical exponent α obtained from Ref. [4] (top panel) and scaling prediction of $\bar{\nu}$ (bottom panel) for 8CB+aerosil samples as a function of the density ρ_S (open circles). In both panels, Tricritical (TC) and XY values are denoted by the horizontal dashed lines. Pure liquid crystal values, obtained from Ref. [23], are plotted versus the McMillan ratio, $R_M \equiv \mathrm{T}_{NA}/\mathrm{T}_{NI}$ (filled circles).

for the N-SmA pseudo-transition for 8CB+aerosil samples can be plotted versus R_M and ρ_S respectively, and this is shown in Fig. 7. In addition, the variation of the mean correlation length exponent $\bar{\nu} \equiv (\nu_{||} + 2\nu_{\perp})/3$ for pure LCs (versus R_M) and those predicted by our two-scale analysis (versus ρ_S) are also plotted. Going from left to right in Fig. 7 corresponds to *decreasing* nematic-smectic coupling along the lines given in Ref. [23] for pure LCs. The two-scale predicted critical evolution of the average correlation length exponent with respect to ρ_S is in good agreement with the corresponding evolution in pure LCs with respect to R_M. This match is completely consistent with the correlation between ρ_S and R_M seen from the experimentally measured exponents α and $x \approx 2\beta$ in Paper I and given previously in Eq. (2). Fig. 7 demonstrates that the two-scale predicted behavior given in this analysis for the correlation lengths is consistent with other observed trends in the evolution of pseudo-critical behavior with ρ_S.

V. DISCUSSION AND CONCLUSIONS

Despite the loss of long-range smectic order, quasi-critical thermal fluctuations remain important at high temperatures for low silica density 8CB+aerosil samples. In addition, two-scale universality analysis provides a link between the SmA quasi-critical behavior of the heat capacity and the correlation lengths. The smectic fluctuations are modified from the pure 8CB behavior due to the effects of quenched-random-disorder. A collection of effective critical exponents for the 8CB+aerosil system and selected pure LCs as a function of ρ_S and R_M, respectively, is presented in Table I. As shown in Paper I and here, the density ρ_S of an aerosil gel is directly correlated to the McMillan ratio R_M of pure LCs, both of which are indicators of the strength of smectic-nematic coupling. The flow of the effective critical behavior for the N-SmA transition shown in Table I and Fig. 7 (see also Fig. 11 of Paper I) as a function of this QRD induced decoupling is consistent with theoretical predictions that no new fixed point is present for the $RFXY$ model [10]. For the liquid crystal - silica dispersion system studied here, the flow is from near a Gaussian tricritical point toward the $3D$-XY fixed point.

This crossover behavior is explained for pure LCs by a decrease in nematic – smectic coupling as R_M decreases. For 8CB+aerosils, an increase in ρ_S appears to have the same effect. Recent work has found that aerosil gels exhibit dynamics which can couple to a host liquid crystal [26] presumably through direct coupling to director fluctuations. Also, recent deuterium NMR studies of 8CB+aerosils [6] found no appreciable change in the magnitude of orientational order above T* for $\rho_S < 0.1$. The reason appears to be that the aerosil particles form a hydrogen-bonded thixotropic $3D$ gel network that provides (a) random anchoring surfaces for 8CB molecules and (b) because of the flexible/fragile nature of the silica

TABLE I: Summary of effective critical exponents for 8CB+aerosils and selected pure LCs taken from Ref. [23]. The McMillan ratio for pure LCs is $R_M = \mathrm{T}_{NA}/\mathrm{T}_{NI}$. Note that ρ_S is given in units of grams of silica per cm^3 of liquid crystal, l_o is in Å, and T* is in Kelvin. The last two columns refer to the fitting parameters for $a_2 = B(\mathrm{T}^* - \mathrm{T})^x$ given in Paper I. Going down the table from XY to Tricritical corresponds to increasing the smectic - nematic coupling. The $\bar{\nu} \equiv (\nu_\parallel + 2\nu_\perp)/3$ entries in square brackets represent the scaling predictions for the 8CB+aerosil samples. For the columns giving $2-\eta$ and x values for 8CB+aerosil samples, the values for $\gamma/\nu_\parallel$ and $2\beta = 2 - \alpha - \gamma$ are given in parentheses for pure liquid crystals.

Sample	R_M	ρ_S	l_o	T*	α	$\bar{\nu}$	$2-\eta$ or $(\gamma/\nu_\parallel)$	x or (2β)	100×B
3*D*-*XY* [25]					−0.013	0.671	1.962	(0.696)	
DB5+C$_5$stilbene	0.780				−0.01	0.62	(1.78)	(0.71)	
7APCBB	0.863				−0.01	0.66	(1.91)	(0.67)	
8CB+sil[12]		0.341	222	304.92			1.83	0.695	6.95
8CB+sil[12]		0.282	262	305.41			2.04	0.65	1.46
4O.7	0.926				−0.03	0.69	(1.87)	(0.57)	
8CB+sil[12]		0.220	328	305.90			1.77	0.60	3.59
8CB+sil[12]		0.161	439	305.54			2.01	0.625	1.13
8CB+sil[12]		0.105	660	306.24			2.08	0.54	2.32
8CB+sil[4]		0.092	748	306.32	−0.02	[0.67]			
8.5S5	0.954				0.10	0.70	(1.90)	(0.42)	
8CB+sil[12]		0.078	882	306.00			1.99	0.465	4.05
8CB+sil[4]		0.052	1306	306.13	0.08	[0.64]			
$\bar{9}$S5	0.967				0.22	0.62	(1.85)	(0.47)	
8CB+sil[12]		0.051	1327	306.24			2.01	0.46	2.36
8CB+sil[12]		0.041	1660	306.28			1.96	0.51	1.08
8CB+sil[12]		0.025	2660	306.15			1.94	0.52	1.18
8CB+sil[4]		0.022	3054	306.23	0.23	[0.59]			
8CB	0.977	0		306.97	0.31	0.56	(1.88)	(0.43)	
$\bar{1}$0S5	0.983				0.45	0.54	(1.80)	(0.45)	
Tricritical					0.50	0.50	2	(0.50)	

gel, random elastic dampening of elastic (director) fluctuations in the liquid crystal. Both effects will reduce the nematic orientational susceptibility by suppressing *director* fluctuations. Thus, increasing ρ_S in LC+aerosil samples is equivalent to decreasing R_M in a pure liquid crystal, which in the case of 8CB drives its critical behavior towards XY. This may have important consequences for the *bulk* N-SmA behavior as theoretical efforts have mostly concentrated on the de Gennes type of smectic coupling to the magnitude of nematic order parameter, and it appears that the coupling to director fluctuations may play an important role in the crossover behavior.

Because the random disorder is introduced by the inclusion of network gel structures within the liquid crystal, finite-size effects can exist and may play a role in truncating thermally driven fluctuations. Such effects would explain the increasing suppression of the heat capacity peak with increasing ρ_S, which corresponds to decreasing the mean distance between solid surfaces. Scaling analysis provides a good description of the maximum heat capacity and the fractional rounding (or truncation) of the transition for all 8CB+aerosil samples. However, FSS analysis does not provide a good prediction of the trend with ρ_S for the transition enthalpy $\delta H_{NA} = \int \Delta C_p(NA) dT$. The reason for this is the fact that the trend in δH_{NA} is dominated not by the truncation of the $\Delta C_p(NA)$ peak but by the changes in shape and size of $\Delta C_p(NA)$ over its entire range, and the latter effect is due to crossover rather than finite-size.

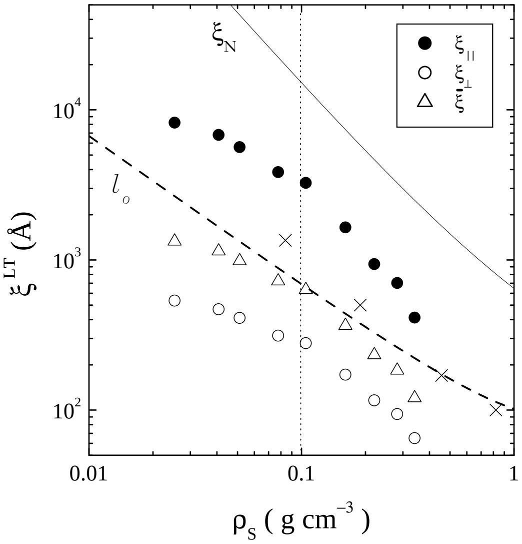

FIG. 8: Saturated 8CB+sil parallel $\xi_\parallel$ (filled circles), perpendicular $\xi_\perp$ (open circles), and mean $\bar{\xi} = (\xi_\parallel \xi_\perp^2)^{1/3}$ (open triangles) smectic correlation lengths ξ^{LT} for T $\ll$ T* versus ρ_S; data taken from Paper I. The low-temperature isotropic smectic correlation lengths ξ reported in Ref. [9] for 8CB+aerogel samples are shown by the × symbols. The solid line is the estimated maximum *nematic* director correlation length ξ_N for 6CB+aerosil [5], and the dashed line is the mean void size l_o estimate given by Eq. (1).

Below the pseudo-transition temperature T*, the correlation lengths and the amplitudes of the thermal term in the smectic structure factor for 8CB+aerosils saturate and are approximately temperature independent [12]. Quenched random disorder imposed by the aerosil gel network dominates the smectic fluctuations below the pseudo-transition. Plotted in Fig. 8 are the low-temperature parallel correlation lengths $\xi_{\|}^{LT}$ taken from Paper I plus the corresponding perpendicular $\xi_{\perp}^{LT}$ values and the mean correlation lengths $\bar{\xi} = (\xi_{\|}\xi_{\perp}^2)^{1/3}$. Also plotted are the "isotropic" smectic correlation lengths reported at low temperature for 8CB+aerogel samples [9], the mean-void size l_o based on Eq. (1), and an estimate of the saturated *nematic director* correlation length ξ_N measured in 6CB+aerosil samples [5]. As discussed in Paper I, the parallel correlation length is much larger than l_o but smaller than ξ_N for all 8CB+aerosil samples studied. The first fact indicates than the smectic domains span many "voids" and it is thus reasonable to expect that their influence is of a random-field type, while the latter fact is physically reasonable since the observed smectic domains cannot be larger than the size of a nematic domain. However, 6CB does not exhibit a smectic phase, so it remains unknown how the director correlation length would change, if at all, due to the onset of smectic order. Interestingly, the low-temperature 8CB+aerogel correlation lengths appear to agree fairly well with l_o, while the aerogel $\Delta C_p(NA)$ peak is severely rounded, indicating that 8CB is very strongly perturbed by the rigid fused silica gel.

In spite of the applicability of the pseudo-critical scaling ideas discussed here and in Paper I, quenched random disorder plays a dominate role in the behavior of 8CB+aerosils for temperatures below T*. In particular, consider the x-ray structure factor below T*, which is dominated by the "Lorentzian-squared" type term expected for random-field disordered systems [12]. Random-field theories postulate a random-field at each i^{th} "spin" site of strength $\vec{h}_i$ whose average is $\langle\vec{h}_i\rangle = 0$ but whose square defines the variance of the disorder $\Delta \equiv \langle\vec{h}_i \cdot \vec{h}_i\rangle = |h^2|$ [27]. The x-ray analysis presented in Paper I uses a structure factor analogous to that used for the analysis of random-field magnets given in Ref. [27]; see Eq. (1) in Paper I, Thus, the saturated (low-temperature, denoted by the superscript LT) values of the mean smectic correlation length $\bar{\xi}^{LT} = (\xi_{\|}\xi_{\perp}^2)^{1/3}$, and the amplitude of the thermal contribution σ_1^{LT}, as well as the amplitude of the QRD contribution a_2 to the structure factor can be compared to the predicted scaling for random-field disorder. Note that a_2 is temperature dependent over the entire temperature range, thus we use a value for $a_2(\Delta T)$ at $\Delta T = T - T^* = -6$ K in what follows. The relevant scaling relations predicted for random-field systems at low temperatures are

$$\begin{aligned} \bar{\xi} &\sim \Delta^{-\nu_\Delta} \\ \sigma_1 &\sim \bar{\xi}^3 \\ a_2 &\sim \bar{\xi}^0 = constant \\ a_2/\sigma_1 &\sim \bar{\xi}^{-3} \end{aligned} \tag{7}$$

where $\nu_\Delta = 1/(d_c - d)$, d_c is the lower critical dimension, and $d = 3$ is the physical dimension of the random-field system [27]. We have dropped the superscript LT for convenience here and in the rest of this discussion. For a pure, continuous symmetry, XY system that exhibit true long-range order $d_c(XY) = 2$, which shifts upward for a random-field XY system to $d_c(RFXY) = 4$ [28]. Although the N-SmA phase transition is not a simple member of the $3D$-XY universality class, Eqs.(7) are expected to be reasonably applicable for smectics. Thus $\nu_\Delta = 1$ for the divergence of the smectic correlation length with the strength of the random-field. Substituting this value of ν_Δ and eliminating $\bar{\xi}$ from the expressions for the scattering amplitudes in Eqs. (7), we find the predicted scaling relations solely in terms of the random-field variance for an $RFXY$ system as

$$\begin{aligned} \bar{\xi} &\sim \Delta^{-1} \simeq |h|^{-2} \\ \sigma_1 &\sim \Delta^{-3} \simeq |h|^{-6} \\ a_2 &\sim \Delta^0 = constant \\ a_2/\sigma_1 &\sim \Delta^3 \simeq |h|^6 \end{aligned} \tag{8}$$

The scaling of these quantities with respect to ρ_S can be compared to the predicted scaling behavior with respect to Δ in order to make a connection between Δ and ultimately $|h|$ with ρ_S. In Paper I the simple assumption that $\Delta \sim \rho_S$ is made, while the assumption $\rho_S \sim |h| \simeq \Delta^{1/2}$ has been made elsewhere [9].

As discussed in Paper I in terms of $\xi_{\|}$, a *one*-regime ρ_S analysis (a single trend over the entire range of ρ_S values studied) yields for the 8CB+aerosil system $\bar{\xi} \sim \rho_S^{-1.0\pm0.2}$. Similarly, the scattering amplitude ratio as a function of $\bar{\xi}$ yields $a_2/\sigma_1 \sim \bar{\xi}^{-2.68\pm0.26}$ at $\Delta T = -6$ K. The scatter in the experimental values of $a_2(\Delta T)$ as a function of ρ_S only allows a very rough estimate of its scaling, but it appears to be very weakly dependent on either correlation length or silica density. Unfortunately, the uncertainties in σ_1^{LT} values arising from fitting the x-rays profiles at low temperatures (where the quenched random term greatly overshadows the thermal fluctuation term) and the added uncertainties from normalization make it unsuitable for testing as a function of ρ_S. However, the ratio $a_2(\Delta T)/\sigma_1^{LT}$ is better characterized since it is independent of the normalization procedure.

One possible explanation for the observed systematic deviations from the simple power-law forms given above is that there is a finite maximum aerosil density above which no smectic correlations can exist. This maximum ρ_S corresponds to a minimum mean void size, l_c, below which the liquid crystal has insufficient space to form smectic layers. Since at low densities the void size l_o is inversely related to ρ_S as shown in Sec. II, we propose an empirical relationship

$$\bar{\xi} = A(l_o - l_c) \tag{9}$$

for a linear scaling of the mean correlation length with the corrected void size $l_o - l_c$. The variation of both $\bar{\xi}$ and $a_2(\mathrm{T}^* - 6\ \mathrm{K})/\sigma_1$ with $(l_o - l_c)$ is given in Fig. 9, where $A \simeq 0.93$ and $l_c \simeq 80$ Å were found by a best linear fit of $\bar{\xi}$ with Eq. (9) [29]. The solid line in the top panel shows the result of this fit. In addition, the solid line in the lower panel of Fig. 9 shows the expected behavior of $a_2(\Delta T)/\sigma_1^{LT}$ given the empirical relationship of Eq. 9 with $l_c = 80$ Å and the random-field scaling predicted in Eq. (8). A fit with $a_2(\Delta T)/\sigma_1^{LT} \sim (l_o - l_c)^y$, allowing y to be a free parameter and fixing $l_c = 80$ Å, yielded the dashed line in the lower panel and the exponent value $y = -2.6$. Since this small l_c value is approximately twice the smectic partial bilayer thickness in 8CB, it is reasonable that no smectic ordering can occur when $l_o \lesssim l_c$. The overall behavior shown in Fig. 9 as compared to the random-field scalings for an XY system suggests that the random-field strength $\Delta = |h|^2 \sim \rho_S$, at least for small ρ_S (and thus large l_o). This use of the empirical relationship in Eq. (9) allows us to bring the observed results into better agreement with predictions for scaling in random-field systems.

There is a second possible explanation for the clear deviations from a simple power-law dependence on ρ_S shown in Paper I and here in Fig. 8. This second possibility is the existence of a more complex relationship between Δ and ρ_S. The correlation lengths appear to have a weaker ρ_S dependence than the mean void size below $\rho_S = 0.1$, while above this density the opposite occurs [30]. In addition, the value of the ratio $a_2(\Delta T = -6\ \mathrm{K})/\sigma_1^{LT}$ exhibits distinctly different power-law dependencies on ρ_S above and below this silica density; see Fig. 10 and also Fig. 12 in Paper I for further details. Using separate power-law characterizations for low density ($\rho_S \leq 0.1$) and high density ($\rho_S \geq 0.1$), we find

$$\begin{aligned} \bar{\xi} &\sim \rho_S^{-0.5\pm0.1}(low\rho_S),\ \sim \rho_S^{-1.4\pm0.1}(high\rho_S) \\ a_2/\sigma_1 &\sim \rho_S^{1.2\pm0.1}(low\rho_S),\ \sim \rho_S^{3.7\pm0.3}(high\rho_S) \end{aligned} \tag{10}$$

These *two*-regime fits are shown for $\bar{\xi}$ and a_2/σ_1 in Fig. 10. Recall that the concept of a low density regime ($\rho_S < 0.1$) and a high density regime ($\rho_S > 0.1$), shown in Eq. (10), is supported by the specific heat data [4], where power-law fits were possible when $\rho_S < 0.1$ but not when $\rho_S > 0.1$.

In order to establish a connection between the disorder variance Δ (a measure of the overall disordering strength of the individual random fields h_i, $\Delta = |h|^2$) and the silica density ρ_S for low and high ρ_S regimes, we compare Eqs. (8) and (10) for $\bar{\xi}$ and the ratio $a_2(\Delta T)/\sigma_1^{LT}$, which are the two best characterized quantities. For $\rho_S \leq 0.1$ the result is $\Delta \sim \rho_S^{0.5}$. In contrast, for $\rho_S > 0.1$ the result is $\Delta \sim \rho_S^{1.3}$. This idea of *two* regimes may be consistent with the picture of the aerosil gel described earlier where, in addition to the random silica strands ("pearl-necklace" of aerosil beads) providing the random-field dictating the local orientation of the nematic director, there perhaps exists an elastic coupling of these tenuous strands to the nematic director. This coupling would dampen the size of director fluctuations analogous to the effect of a wider nematic temperature range, and this gives a physical interpretation to the critical flow with random-field strength towards the underlying XY fixed point. The apparent increase in the *relative* effect of the elastic coupling seen by the stronger scaling of the quenched random disorder strength with silica density may be an indication that the aerosil gel has become significantly stiffer when $\rho_S > 0.1$ suggesting the possibility that a rigidity transition has occurred in the gel.

In conclusion, a combination of finite-size effects and two-scale universality concepts has yielded a successful connection between 8CB+aerosil thermal behavior and x-ray correlation length behavior. The truncation of $\Delta C_p(NA)$ peaks, measured by h_M and $\delta\mathrm{T}^*/\mathrm{T}^*$, and the observation of high-temperature 8CB+aerosil correlation lengths that are close to those for pure 8CB are both well explained. The observed dependence of the integrated area δH_{NA} on ρ_S is not properly described by

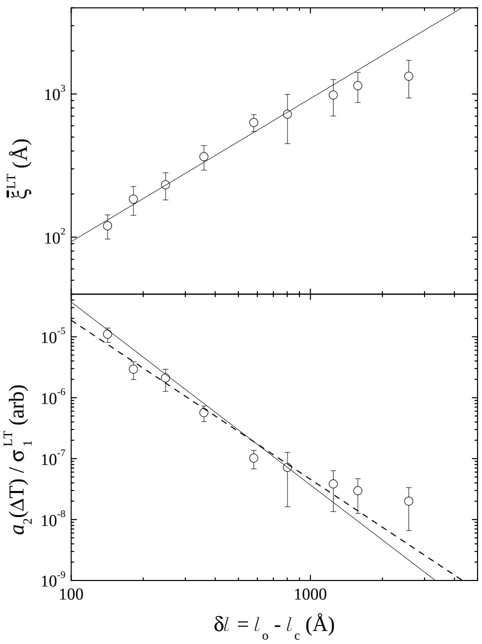

FIG. 9: The low-temperature mean smectic correlation length $\bar{\xi} = (\xi_\parallel \xi_\perp^2)^{1/3}$ (top panel) and scattering amplitude ratio a_2/σ_1 (bottom panel) for 8CB+aerosil versus $\delta l = (l_o - l_c)$; data taken from Paper I. The lower critical length-scale below which not even short-range smectic order survives is $l_c \simeq 80$ Å. The solid lines depict the empirical trend $\bar{\xi} \sim \delta l$ and the $a_2(\Delta T = -6\ \mathrm{K})/\sigma_1^{LT} \sim \delta l^{-3}$ trend expected for random-field scaling. The dashed line in the lower panel indicates a free fit with $a_2/\sigma_1 = C(l_o - 80\ \text{Å})^y$, where the value $y = -2.6$ was obtained.

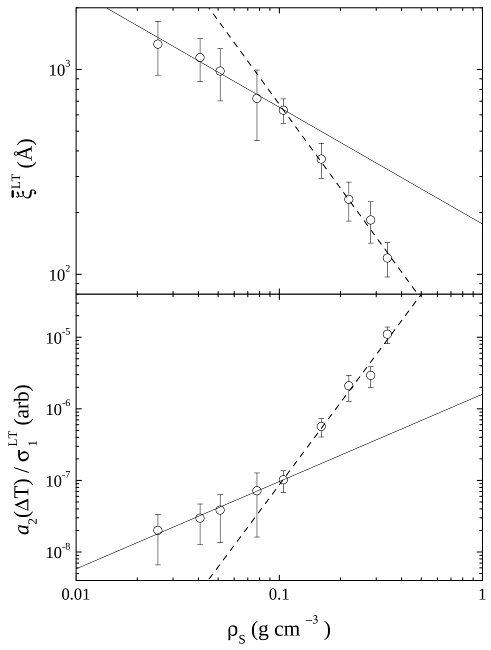

FIG. 10: The low-temperature mean smectic correlation length $\bar{\xi} = (\xi_{\|}\xi_{\perp}^2)^{1/3}$ (top panel) and scattering amplitude ratio $a_2(\Delta T = -6\text{ K})/\sigma_1^{LT}$ for 8CB+aerosil versus ρ_S; data taken from Paper I. The solid and dashed lines depict the low and high density regimes, respectively, with slopes given in Eq. (10).

finite-size scaling, and the reason for this failure is clear. Trends in $\delta H_{NA}(\rho_S)$ reflect the changing shape of ΔC_p peaks over a wide temperature range as ρ_S varies. As described in Paper I [12] and in Sec. IV of the present paper, quenched random disorder plays a dominant role in changing the effective pseudo-critical exponents that describe the smectic behavior in 8CB+aerosils. The density ρ_S for 8CB+aerosil samples can be equated to the McMillan ratio R_M for pure LCs; see Eq. (2). Since in pure LCs a larger McMillan ratio implies a larger nematic susceptibility, increasing R_M corresponds to increasing the smectic-nematic coupling. Increasing ρ_S for LC+aerosils has the opposite effect, as expected. The linearity of the relationship between ρ_S and R_M provides support for the view that the aerosil gel is involved in decoupling the nematic and smectic order parameters. It seems possible that the elasticity of the aerosil gel plays an important part in the theory of gels as a random perturbation acting on the N-SmA transition in liquid crystals. Theory incorporating such elastic aspects is in progress [15]. Finally, reasonable scaling was observed of the smectic correlation length and scattering amplitudes with respect to the silica density or mean void size, which were roughly consistent with predictions for random-field type disorder. However, the theoretical predictions for random-field systems were for uncorrelated random fields, while the disorder due to the aerosil gel are correlated, over some small length scale, due to their fractal structure [31]. The effect of algebraic correlations in the disorder on the random-field scaling predictions would be an attractive avenue for theoretical investigation.

Acknowledgments

We thank P. Clegg, T. Bellini, L. Radzihovsky, N. A. Clark, and A. Aharony for helpful discussions. This work was supported by the NSF under the NSF-CAREER award DMR-0092786 (WPI), the NSF-CAREER award DMR-0134377 (JHU), and Contract No. DMR-0071256 (MIT) and by the Natural Science and Engineering Research Council of Canada (Toronto).

APPENDIX A: RELEVANT NEMATIC - SMECTIC-A BEHAVIOR IN PURE LIQUID CRYSTALS

1. General Description of the N-SmA phase transition

Although there is still some theoretical debate, the best experimental evidence to date points to $3D$-XY as the underlying critical behavior for the N-SmA transition over experimentally accessible ranges of reduced temperature t [32]. For pure liquid crystals, smectic ordering is strongly influenced by two types of coupling to nematic order: coupling to the magnitude of nematic order (S) and to the nematic director fluctuations ($\delta\hat{n}$).

2. Smectic coupling to the nematic order parameter

The first type of nematic - smectic coupling is the so-called de Gennes coupling of the form $\psi^2 S$. Such a term affects the coefficient b of the quartic term $b\psi^4$ in the mean-field Landau expansion of the smectic free-energy in terms of the complex smectic order-parameter ψ [33]. Since the nematic elastic constants are proportional to the square of S, this coupling reflects the effect of the "softness" of the nematic order prior to the onset of smectic order. The strength of this coupling depends on the magnitude of the nematic susceptibility, χ_N, and such a coupling can drive the N-SmA transition from XY-like ($b \gtrsim 0$) to TC ($b = 0$) to weakly first-order ($b < 0$) with increasing χ_N. This is clearly seen as a trend with the width of the nematic temperature range, or the McMillan ratio $R_M = \text{T}_{NA}/\text{T}_{NI}$, which directly influences χ_N [23]. As an example, the heat capacity critical exponent varies from $\alpha = 0.50$ to 0.10 as this ratio varies from $R_M = 0.994$ for a 2-K wide nematic range to ~ 0.954 for a 15-K wide nematic range. For LC samples with large nematic ranges, $R_M \approx 0.898$ (45-K wide) to $R_M \approx 0.660$ (189-K wide), the experimental exponent is $\alpha \approx \alpha_{XY} = -0.013$ [25, 34].

3. Smectic coupling to director fluctuations

Smectic order coupling to the director fluctuations has the form $\psi^2\delta\hat{n}$. Thus, in addition to the "softness" of the nematic, fluctuations in the director orientation compete with the establishment of smectic order by exciting anisotropic elastic deformations in the smectic. The theory for such coupling is not yet complete nor are all the implications of this effect understood, but a self-consistent one-loop model has been put forward [35]. This type of coupling leads to anisotropy in the correlation lengths parallel and perpendicular to the nematic director (a feature not present in a normal $3D$-XY system) and a very gradual crossover from a broad weakly-anisotropic critical correlation regime $\nu_{||} \geq \nu_{\perp}$ (weak coupling limit) toward a strongly-anisotropic $\nu_{||} = 2\nu_{\perp}$ regime (strong coupling limit). The strength of this coupling depends on the magnitude of the splay elastic constant K_{11}, which should vary as $K_{11} \sim S^2$. Note that the XY model has no such splay component. Thus, a liquid crystal with a small nematic range will have a small K_{11} at T_{NA} and should lie deep in the anisotropic crossover regime. Liquid crystals with a large nematic range will have a relatively large K_{11} at their T_{NA} and should straddle isotropic and weak-anisotropic regimes. The latter is observed experimentally, but strong anisotropy, $\nu_{||} = 2\nu_{\perp}$, is not seen for any smectic since the narrow nematic range condition also induces the de Gennes coupling and thus crossover to tricritical and even first-order behavior [23].

APPENDIX B: SCALING BACKGROUND

1. Finite-size scaling

The concept of finite-size effects is a straightforward and basic idea in the modern theory of phase transitions [36, 37]. Ignoring specific surface interactions, finite-size effects stem from the saturation upon cooling of the growing correlation length in a disordered phase to a finite length scale. In traditional finite-size scaling (FSS), the maximum length is dictated by the "container" size. This effect truncates the transition prematurely and leads to three observable effects on the calorimetric data: a suppressed heat capacity maximum, a rounding of the transition in temperature, and a suppression of the transition enthalpy. In addition, for a transition that breaks a continuous symmetry, random-fields lead to a saturation in the growth of order. The hypothesis dictating our approach is that the same analysis can be applied in the case of either type of truncation, provided changes in the critical behavior due to the disorder are accounted. In the case of random-fields, we call this analysis random-field scaling (RFS).

In order to proceed, the power-law behavior of the smectic correlation length in the nematic phase needs to be considered. It is common practice to ignore corrections-to-scaling terms and use simple pure power laws although this is inconsistent with theory as discussed in Ref. [32]. The correlation lengths of pure LCs are anisotropic with respect to the smectic layer normal (i.e., the nematic director for smectic-A phases) and are represented by effective critical exponents that are free parameters [24, 32]

$$\xi_{||} = \xi_{||o} t^{-\nu_{||}} \tag{B1}$$

$$\xi_{\perp} = \xi_{\perp o} t^{-\nu_{\perp}} \tag{B2}$$

where $\xi_{||o}$ and $\xi_{\perp o}$ are the bare correlation lengths and $\nu_{||}$ and $\nu_{\perp}$ are the exponents parallel and perpendicular to the layer normal, respectively.

For smectic liquid crystals, the parallel correlation length is always larger than the perpendicular, and so our analysis uses this length scale for the definition of the minimum reduce temperature. Defining the maximum possible correlation length as ξ_M, one solves Eq. (B1) for the *minimum* reduced temperature above T* as $t_m^+ = (\xi_M/\xi_{||o})^{-1/\nu_{||}}$. It is not possible to define a similar minimum reduced temperature below the transition since the critical correlation length behavior below T* is not known. Thus, the equation for the fractional rounding (truncation) of the transition due to finite length effects is estimated to be

$$\delta T^*/T^* = (|t_m^+| + |t_m^-|) \approx 2t_m^+ = 2(\xi_M/\xi_{||o})^{-1/\nu_{||}} \ . \tag{B3}$$

Substituting t_m^+ into Eq. (3) gives the relationship for the heat capacity maximum h_M at the N-SmA transition as

$$h_M = A^{\pm}(\xi_M/\xi_{||o})^{\alpha/\nu_{||}}(1 + D^{\pm}(\xi_M/\xi_{||o})^{-\Delta_1/\nu_{||}}) + B_c \ . \tag{B4}$$

Because of the importance of corrections-to-scaling for the analysis of $\Delta C_p(NA)$, a log-log plot of $h_M - B_c$ versus ξ_M would not yield a straight line of slope $\alpha/\nu_{||}$. The FSS effect on the N-SmA transition enthalpy is obvious since it involves replacing the singular $\Delta C_p(NA)$ peak between t_m^+ and t_m^- by h_M and thus decreasing the integral of $\Delta C_p(NA)$ over T.

2. Two-scale universality for T > T*

Two-scale theory of critical phenomena relates the non-universal coefficient of the heat capacity's leading singularity to the non-universal bare correlation volume [25, 38], and it also yields the hyperscaling relation between the critical exponents α and ν. For liquid crystals, there is an anisotropic version of hyperscaling [39]

$$2 - \alpha = \nu_{||} + 2\nu_{\perp} \ , \tag{B5}$$

which is empirically supported by the somewhat scattered available data on pure LCs like 8CB [23]. If such hyperscaling holds, then a two-scale relation can be written as

$$\alpha A^{+}(\xi_{\|o}\xi^2_{\perp o}) = k_B(R^{+}_{\xi})^3 = 13.8(R^{+}_{\xi})^3 \ , \qquad \text{(B6)}$$

where k_B is the Boltzman constant and the value 13.8 pertains when the correlation lengths are in units of Å and A$^+$ is in units of J K^{-1} g^{-1}. The quantity R^{+}_{ξ} has a different universal value for each universality class. For the 3*D*-*XY* model, the value of $13.8(R^{+}_{\xi})^3$ is 0.647 [25] and several pure LCs have been shown to have $\alpha A^{+}(\xi_{\|o}\xi^2_{\perp o})$ values close to this [32]; the value for 8CB is 0.651 [4, 24]. Assuming that hyperscaling and XY-like pure LC values of R^{+}_{ξ} hold for 8CB+sil samples independent of ρ_S, then

$$\alpha A^{+}(\xi_{\|o}\xi^2_{\perp o}) \simeq 0.647 \ . \qquad \text{(B7)}$$

Thus, heat capacity critical behavior (α and A$^+$ values) for LC+aerosils will allow the determination of $\nu_{\|} + 2\nu_{\perp}$ and $(\xi_{\|o}\xi^2_{\perp o})$.

---

[1] M. Chan, N. Mulders, and J. Reppy, Physics Today **49**, 30 (1996), and references therein.

[2] Q. J. Harris, Q. Feng, Y. S. Lee, R. J. Birgeneau, and A. Ito, Phys. Rev. Lett. **78**, 346 (1997), and references therein.

[3] B. Zhou, G. S. Iannacchione, C. W. Garland, and T. Bellini, Phys. Rev. E **55**, 2962 (1997).

[4] G. S. Iannacchione, C. W. Garland, J. T. Mang, and T. P. Rieker, Phys. Rev. E **58**, 5966 (1998).

[5] T. Bellini, N. A. Clark, V. Degiorgio, F. Mantegazza, and G. Natale, Phys. Rev. E **57**, 2996 (1998).

[6] T. Jin and D. Finotello, Phys. Rev. Lett. **86**, 818 (2001).

[7] M. Marinelli, A. K. Ghosh, and F. Mercuri, Phys. Rev. E **63**, 061713 (2001).

[8] S. Park, R. L. Leheny, R. J. Birgeneau, J.-L. Gallani, C. W. Garland, and G. S. Iannacchione, Phys. Rev. E **65**, 050703(R) (2002).

[9] T. Bellini, L. Radzihovsky, J. Toner, and N. A. Clark, Science **294**, 1074 (2001).

[10] A. Pelissetto and E. Vicari, Phys. Rev. B **62**, 6393 (2000).

[11] L. Radzihivsky and J. Toner, Phys. Rev. B **60**, 206 (1999).

[12] R. L. Leheny, S. Park, R. J. Birgeneau, J.-L. Gallani, C. W. Garland, and G. S. Iannacchione, Phys. Rev. E (2002), preceding paper, denoted as Paper I.

[13] P. D. Olmsted and E. M. Terentjev, Phys. Rev. E **53**, 2444 (1996).

[14] S. P. Meeker, W. C. K. Poon, J. Crain, and E. M. Terentjev, Phys. Rev. E **61**, R6083 (2000).

[15] L. Radzihovsky, private communications.

[16] Degussa Corp., Silica Division, 65 Challenger Road, Ridgefield Park, NJ 07660. Technical data given in the Degussa booklet AEROSILS.

[17] R. Leheny, D. Liang, A. Roshi, and G. Iannacchione, unpublished.

[18] H. Sonntag and K. Strenge, *Coagulation Kinetics and Structure Formation* (Plenum Press, New York, 1987), pp. 134–145 and 172–177.

[19] G. Porod, *Small Angle X-ray Scattering* (Academic Press, 1982), chap. 2, pp. 18–51, eds. O Glatter and O Kratky.

[20] L. Wu, B. Zhou, C. W. Garland, T. Bellini, and D. W. Schaefer, Phys. Rev. E **51**, 2157 (1995).

[21] Together with the overall density of solid, ρ = mass of solid per total sample volume, and the density of the solid itself, ρ_M = mass of solid per solid volume (2.2 g cm^{-3} for silica) where $\rho^{-1} = \rho_S^{-1} + \rho_M^{-1}$, other gel parameters may be determined. Note that as ρ varies from zero (no solids present) to its maximum of ρ_M (all solids, no open volume), ρ_S varies from zero ($l_o \to \infty$, or sample size) to infinity ($l_o \to 0$, or no open volume). The solid volume fraction is given by $\Phi = \rho/\rho_M$ while the open volume fraction, or porosity, is given by $\phi = 1 - \Phi = \rho/\rho_S$.

[22] Note that only over some, as yet not well defined, range of solids concentration can an increase in Φ be considered an increase in the "strength" of the quenched disorder. In reality, the surface interactions between the material filling the voids and the solid surfaces are dictated by the materials themselves and remain constant. Since liquid crystals are quite "soft" materials elastically, the quenched state of molecules at a surface decays relatively slowly away from the surface. Thus, a point will occur where $p < 1$ and yet everything between the surfaces can be considered quenched. In general, increasing Φ for large values of Φ only increases the extent of the surfaces and so the extent of the disorder but not its strength.

[23] C. W. Garland and G. Nounesis, Phys. Rev. E **49**, 2964 (1994).

[24] B. Ocko, R. J. Birgeneau, and D. Lister, Z. Phys. B **62**, 487 (1986).

[25] M. Campostrini, A. Pelissetto, P. Rossi, and E. Vicari, Phys. Rev. B **62**, 5843 (2000).

[26] C. C. Retsch, I. McNulty, and G. S. Iannacchione, Phys. Rev. E **65**, 032701 (2002).

[27] A. Aharony and E. Pytte, Phys. Rev. B **27**, 5872 (1983).

[28] A. Aharony, Y. Imry, and S. Ma, Phys. Rev. Lett. **37**, 1364 (1976).

[29] Our confidence of a linear relationship between $\bar{\xi}$ and l_o can be tested by a free fit with $(l_o - l_c)^z$ with $l_c = 80$ Å. Fitting all the data finds $z = 0.90 \pm 0.12$ while excluding the lowest ρ_S point gives $z = 0.96 \pm 0.11$. .

[30] An interesting feature of the $\bar{\xi}$ behavior is that at $\rho_S = 0.1$, it is nearly equal to l_o. This suggests that the number density of smectic domains, $\bar{\xi}^{-3}$, is growing at a slower rate than the number density of voids, l_o^{-3} with increasing silica density until at $\rho_S = 0.1$, where there exists, on average, one smectic domain for each void. With increasing silica density above $\rho_S = 0.1$, the number density of smectic domains is growing much faster than the number density of voids indicating the stronger disordering effects of the silica gel for these concentrations.

[31] A. Aharony, private communications.

[32] C. W. Garland, G. N. Nounesis, M. J. Young, and R. J. Birgeneau, Phys. Rev. E **47**, 1918 (1993).

[33] P. G. de Gennes and J. Prost, *The Physics of Liquid Crystals* (Clarendon Press, Oxford, England, 1993), 2nd

ed.
[34] J. A. Lipa, D. R. Swanson, J. Nissen, T. C. P. Chui, and U. E. Israelson, Phys. Rev. Lett. **76**, 944 (1996).
[35] B. S. Andereck and B. R. Patton, Phys. Rev. E **49**, 1393 (1994).
[36] M. N. Barber, *Finite-size scaling* (Academic Press, London, 1983), vol. 8, chap. 2, pp. 145–477.
[37] K. Binder, Annu. Rev. Phys. Chem. **43**, 33 (1992).
[38] C. Bagnuls and C. Berviller, Phys. Rev. B **32**, 7209 (1985).
[39] T. C. Lubensky, J. Chim. Phys. **80**, 31 (1983), and references cited therein.